Distributed LSTM-GCN based spatial-temporal indoor temperature prediction in multi-zone buildings

Abstract—Indoor temperature prediction of multiple zones in near future horizons is vital in developing an optimal regulation strategy of Heating, Ventilation, and Air Conditioning systems in large-scale complex buildings. This is however challenging due to the spatial-temporal correlation and multivariable coupling characteristics. This paper proposes a novel deep learning framework incorporating the distributed Long Short-Term Memory and Graph Convolution Network namely DL-GCN for indoor temperature prediction in large public buildings, aiming to learn the spatial-temporal correlation and multivariable coupling features. Firstly, the indoor temperature and humidity data from different zones are handled by GCN networks to extract the temperature spatial features. Then in the distributed LSTM module, other data such as light and AC power consumption are fused with the outputs of the GCN module respectively in a distributed way to learn the coupling interactions and temporal characteristics between these variables. Comparison study and ablation experiments are conducted using real datasets from a large-scale building to verify its effectiveness and superior performance in multi-zone indoor temperature prediction.

Index Terms—Temperature prediction, graph convolutional neural networks, long short-term memory networks, spatial-temporal modeling.

NOMENCLATURE

Symbols

A	Adjacent matrix
$\hat{A}$	The learned Adjacent matrix
E	Graph edges set
E_1, E_2	source and target node embeddings
G	Graph
G^l	the output of l-th spectral convolution layer
g_θ	Filter function in GCN
H_{t-h}^{fusion}	Coupling correlation between temperature and humidity
H_{t-l}^{fusion}	Coupling correlation between temperature and light
H_{t-AC}^{fusion}	Coupling correlation between temperature and AC
$H_{overall}^{fusion}$	Overall coupling correlation between temperature and other auxiliary variables
H^{fusion}	Output of the distributed information fusion module
$\mathbf{L}$	normalized graph Laplacian
N	Graph nodes number
U	Matrix of eigenvectors of the normalized graph Laplacian
V	Graph nodes set

$\mathbf{x}^{t,temp}$	Temperature vector at time t
$\mathbf{x}^{t,h}$	Humidity vector at time t
$\mathbf{x}^{t,light}$	Light use vector at time t
$\mathbf{x}^{t,AC}$	AC consumption vector at time t
$\mathbf{X}^t$	Data matrix at time t
$\mathbf{X}_{temp}^{GCN}$	Temperature spatial features from GCN
MAE	Mean Absolute Error
MSE	Mean Square Error
$CORR$	correlation coefficient
$\lambda_{\max}$	maximum eigenvalue in L
θ	Filter parameter vector
Λ	The diagonal matrix of eigenvalues

I. INTRODUCTION

THE energy consumption of Heating, Ventilation, and Air Conditioning (HVAC) systems in buildings has attracted much attention in recent years due to their increasing rate of power usage and heat electrification of buildings [1], [2]. Advanced energy management of the HVAC systems is vital to achieve energy savings by timely identifying the most energy efficient operating points of the equipment or optimizing the whole system advanced approaches such as the model predictive control (MPC) [3] and deep reinforcement learning [4], etc. And effective indoor air temperature prediction in the near future time horizons is helpful in developing an effective and efficient control strategy of the HVAC system. For example, for energy-saving control of HVAC with advanced techniques, such as model predictive control, the values of the indoor air temperature from the near future are often used in finding the optimal control action of the HVAC equipment. However, it is a challenge to build an accurate dynamic predictive model of indoor temperature due to transportation delays and distributed nature of temperature, especially for large public and commercial buildings with multi-zones.

Previous studies in temperature prediction can be roughly classified into three major categories, namely physics-based approaches, statistical methods and machine learning methods. In physical-based approaches, physical and material properties, and thermal balance equations for buildings are required to achieve good prediction performance. It is hard and time-consuming to collect all required information in detail, particularly for large public and commercial buildings [5]. Statistical methods, such as Autoregressive Integrated Moving Average (ARIMA) [6] are widely used in indoor temperature prediction. However, the effects of statistical methods are limited

when dealing the multi-zone temperature with nonstationary and nonlinear characteristics [7], [8]. To address this problem, machine learning methods, such as Artificial Neural Networks (ANNs) [9], Neuro-fuzzy model [10] and Extreme Learning Machine (ELM) [11] have been viewed as promising tools. Yet, these traditional shallow network based machine learning tools are still not sufficiently effective when applied to indoor temperature prediction for large public and commercial buildings where the features of multivariable coupling, and spatial, and temporal correlation are significant [12]–[14].

The recent mass applications of Internet of Things (IoT) and smart sensors have made it feasible to acquire the real-time time-series measurements of indoor temperature in buildings at a low cost. Thus, it becomes realistic to train deep learning models for multi-zone indoor air temperature prediction instead of shallow network based models [15]. Extensive researches have been conducted on temperature prediction using LSTM. For instance, Fang et al. presented an LSTM-based sequence to sequence model to predict multizone indoor temperature with improved performance over some existing advanced models [16].Xu et al. [17] used an error correction model to improve the short-term indoor temperature prediction accuracy of an LSTM model.

Most of the aforementioned approaches primarily aim to capture temporally correlated information of indoor temperature, e.g., external weather information and historical values of indoor temperature [18] while the spatial correlation is ignored by large. Recently, spatial correlation model methods, such as Graph Convolution Networks (GCN) have been used in traffic flow forecasting [8], [19], [20], air quality forecasting [21], wind speed forecasting [22], etc. In large public and commercial buildings, the temperature variation behaviors differ from time to time, zone to zone due to the diversity of room functions, thermal loads, orientations, and floors, etc. [23]. The spatial-temporal correlation extraction is a critical step for accurate indoor temperature prediction in large public and commercial buildings. In this paper, a novel end-to-end deep learning architecture that incorporates distributed LSTM and GCN named DL-GCN is proposed to capture the multivariable spatial-temporal coupling correlation information for indoor temperature prediction in large public and commercial buildings. The key contributions of this work are summarized as follows:

1) Spatial information extraction with GCN: the spatial dependency between multiple zones are as the first ever attempt considered when developing the indoor air temperature predicting model in large public and commercial buildings. The GCN is used to extract the spatial features of the multiple-zone temperatures from the historical data directly without additional a prior knowledge.

2) Multivariable coupling feature extraction: the coupling and nonlinear characteristics are extracted from the multiple variables (e.g. temperature, humidity, lights, and air conditioning power consumption) that affect the indoor temperature, and the distributed fusion technology is implemented. The multi-zone temperature prediction accuracy is improved with the spatial and temporal information fused in a distributed manner.

3) New model architecture: a novel model architecture named DL-GCN is proposed to capture the multivariable spatial-temporal coupling correlation. To further validate the performance of the proposed DL-GCN model, extensive experiments are conducted using real-world datasets and the experimental results confirm the performance of the proposed approach. The model architecture can provide an effective solution when handling the time series prediction problem with multivariable spatial-temporal coupling correlation.

The remainder of this paper is organized as follows. Section II introduces the multivariable spatial-temporal coupling of multi-zone indoor temperature in large public and commercial buildings. Section III presents some preliminaries and problem formulation. Section IV gives the details of the proposed DL-GCN model. Section V presents the experimental study and discusses the results. Finally, Section VI concludes the paper.
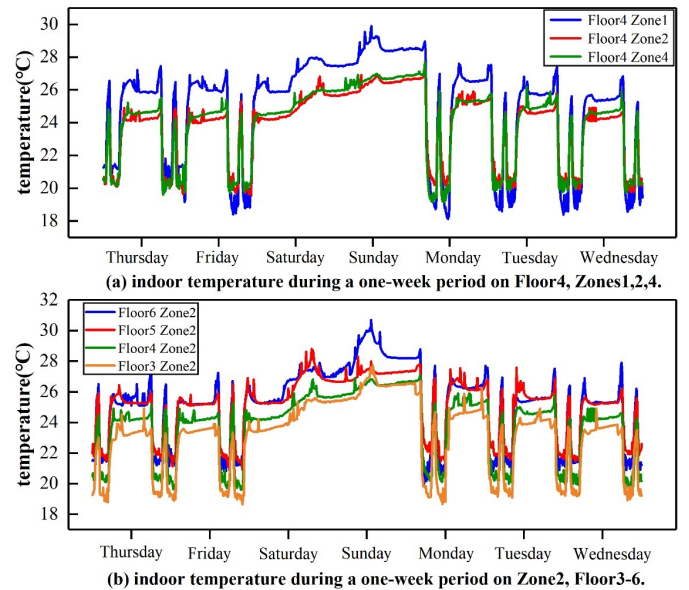

(a) indoor temperature during a one-week period on Floor4, Zones1,2,4.

(b) indoor temperature during a one-week period on Zone2, Floor3-6.

Fig. 1. The trend of indoor temperature during one week.

II. MOTIVATIONS

This section mainly introduces the characteristics of multi-zone indoor temperature distribution in large public and commercial buildings where the multivariable spatial-temporal coupling exist which presents a major challenge for accurate multi-zone indoor temperature forecasting.

A. Spatial and Temporal correlation

The temperature variation patterns are similar in general but the values are different from time to time, and zone to zone, in large-scale buildings due to the diversity of room functions, thermal loads, orientations, and floors. etc. We take one week's temperature profiles from a large-scale building datasets (CU-BEMS) to analyze the temporal and spatiotemporal properties of the indoor temperature, as shown in Fig. 1 [24]. The indoor temperatures vary over time with similar temporal

patterns in one day for different zones, which implies that the indoor temperature of the previous moments can help to predict future temperature due to the temporal feature. From day to day, the temperature profile changes periodically on working days, but the pattern is quite different on the weekends. Moreover, similar spatiotemporal patterns can also be observed in different zones on the same floor. The floor plans of a large building is shown in Fig. 2 [24]. For example, the temperature in zone 2 on floor 4 has a similar trend to zone 4, but it is quite different from zone 1 though zone 1 is closer to zone 2 on the same floor. Additionally, diverse temperature trajectories exist between floors. From Fig. 1(b), the changing patterns are similar but with different values for the same zone (zone 2) from different floors (3, 4, 5, and 6). The temperatures are higher for floors 5 and 6 due to more sunlight and hence more hot air compared with the other lower floors. Hence, the temporal and spatiotemporal properties of building indoor temperature are complex and affected not only by the simple cyclical pattern or topological structure of the building. Spatial-temporal features, such as the recent historical temperatures, periodicity with varying peaks, indoor occupants' behaviors, neighboring zones' conditions, zone layout, etc., should also be considered to achieve more accurate temperature prediction results for large-scale buildings.
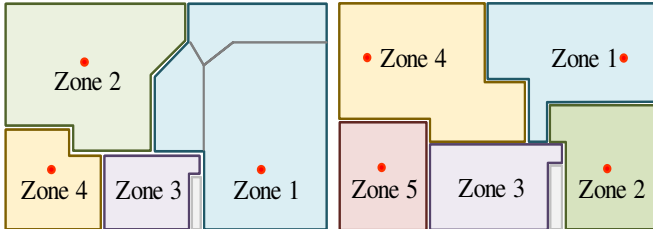

Fig. 2. Floor plans on Floors 1–2 (left) and Floors 3–7 (right). Red dots illustrate the multi-sensors existing in this zone.

B. Multivariable Coupling Phenomenon

The indoor temperature for a single zone is influenced by both various factors. The indoor temperature at different times, as a temporal sequence, is directly related to some recent historical values. Moreover, other contributing factors, such as indoor relative humidity, on/off states of AC and lighting also have influence on the future changes of the indoor temperature. Take the usage of HVAC equipment as an example, the indoor temperature, humidity, and electricity consumption of AC units in zone 4 on Floor 5 during one day are shown in Fig. 3. It is shown that the indoor temperature drops to about 24°C during the periods of 9:30 to 12:00, 14:00 to 18:00 when the AC unit operates while the relative humidity decreases correspondingly. Meanwhile, both the temperature and relative humidity are fluctuating with the on/off, high-level, and medium-level usage of the AC unit. From 12:30 to 14:00, and after 20:00, the AC unit is turned off during lunch break and off office time, both the indoor temperature and relative humidity are rising due to the heat and moisture transferred into the zone. Moreover, it is well understood

that air relative humidity is coupled with temperature by the saturated vapor pressure. Therefore, the indoor temperature is influenced by multiple coupling variables. The extraction of useful information considering the coupling among multiple variables will help to improve the prediction accuracy of indoor temperature.

In summary, there exist multivariable spatial-temporal coupling correlations characteristics for the indoor temperature in large public and commercial buildings, and innovative deep learning frameworks are needed to handle such complex issues and offer better prediction accuracy for multi-zone large-scale buildings.

III. PRELIMINARIES

The multi-zone indoor temperature prediction of public and commercial buildings can be considered as a multivariable coupling spatial-temporal series prediction problem. The graph network is a powerful approach to describe the space layout. This section will introduce the relevant terminologies for multivariate time series forecasting and formulate the temperature spatial-temporal forecasting problem as follows.

Definition 1 (Definition of Graph Network): We construct a graph $G = (V, E)$ to describe the zone layouts and the interactions between them in the public building, where V represents a set of nodes, and E denotes a set of edges. Each represents a zone node from N nodes and $e \in E$ denotes the interactions between a pair of nodes. An adjacency matrix is used to describe the connections for each pair of nodes, denoted as $A \in R^{N \times N}$. If node i and node j are directly connected then the matrix element $A_{ij} > 0$, otherwise $A_{ij} = 0$.

Definition 2 (Data Structure): The current and historical observations of indoor temperature and related variables (e.g., humidity, lighting conditions, AC power consumption) from multiple zones and floors are handled with *Graph-based Data Structure*. At every sampling time t, data vector $\mathbf{x}^{t,temp} = (x_1^{t,temp}, x_2^{t,temp}..., x_{mF}^{t,temp})^{\mathbf{T}} \in \mathbb{R}^{mF \times 1}$ is obtained to describe the measured temperature values for the m zones in each floor, and F floors. Similarly, $\mathbf{x}^{t,h} = (x_1^{t,h}, x_2^{t,h}, ..., x_{mF}^{t,h})^{\mathbf{T}} \in \mathbb{R}^{mF \times 1}$, $\mathbf{x}^{t,light} = (x_1^{t,light}, x_2^{t,light}, ..., x_{mF}^{t,light})^{\mathbf{T}} \in \mathbb{R}^{mF \times 1}$, $\mathbf{x}^{t,AC} = (x_1^{t,AC}, x_2^{t,AC}, ..., x_{mF}^{t,AC})^{\mathbf{T}} \in \mathbb{R}^{mF \times 1}$ represent the values of relative humidity, light, and AC power consumption from the zones, respectively. Thus, the observations for the multiple zone temperature at every sampling time t can be denoted as a data matrix, $\mathbf{X}^t = (\mathbf{x}^{t,temp}, \mathbf{x}^{t,h}, \mathbf{x}^{t,light}, \mathbf{x}^{t,AC}) \in \mathbb{R}^{mF \times 4}$.

Definition 3 (Problem Statements): Following the above definitions, given a sequence for the past T_h historical spatial-temporal input data, the multi-zone indoor temperature prediction problem can be formulated as learning a function $F(\cdot) : \mathbb{R}^{T_h \times mF \times 4} \rightarrow \mathbb{R}^{mF \times 4}$ that maps the input data $\{\mathbf{X}^{t-T_h+1}, \cdots, \mathbf{X}^t\}$ to the temperatures of $m \times F$ zones at the next time step. The problem is defined mathematically as:

$$\{\mathbf{X}^{t-T_h+1}, \mathbf{X}^{t-T_h+2}, ..., \mathbf{X}^t, G\} \xrightarrow{F(\cdot)} \mathbf{x}^{t+1,temp} \qquad (1)$$
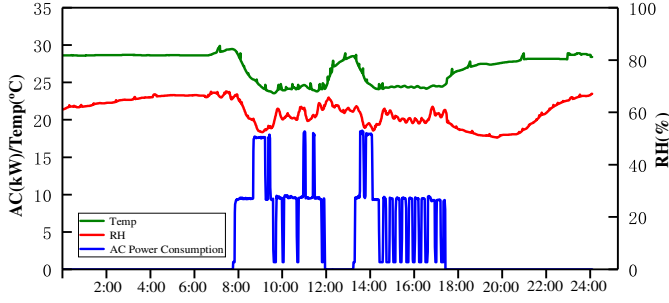
Fig. 3. AC power consumption, indoor temperature, and humidity during one-day period (2019.08.06) on Floor 5, zone 4.

IV. SPATIAL-TEMPORAL MODELLING METHODOLOGY

Focusing on the aforementioned multi-zone indoor temperature prediction problem in a large public and commercial building, a novel end-to-end model, namely DL-GCN is proposed in this section. The modeling process of DL-GCN has two steps, namely spatial features extracted by GCN and temporal features extracted by distributed LSTM network, as shown in Fig.4. In the first step, the multi-zone indoor temperature and humidity data from each zone and floor are handled by a GCN network to extract the spatial features, respectively. A graph learning module is adopted to update the adjacent matrix of the GCN so that the hidden internal dependencies between the zones and floors can be updated adaptively during the training process. In the second step, the other original data such as light and AC power consumption are fused with the outputs of the GCN module respectively in a distributed way, and then processed with the LSTM modules, to learn the multivariable coupling interactions and temporal characteristics.

A. Spatial Features Extraction by GCN

To capture the spatial correlation features of multi-zone indoor temperature, a GCN with graph learning module to adaptively update the adjacency matrix, is proposed. In the GCN, the spectral convolutions [25] are applied on graphs as the input temperature data $\mathbf{x}^{t,temp} \in \mathbb{R}^{mF \times 1}$ with a filter $g_\theta = diag(\theta)$ parameterized by $\theta \in \mathbb{R}^{mF \times 1}$,

$$g_\theta * \mathbf{x}^{t,temp} = Ug_\theta U^T \mathbf{x}^{t,temp} \tag{2}$$

where θ is the parameter of the filter. U is the matrix of eigenvectors of the normalized graph Laplacian $L = I_{mF} - D^{-\frac{1}{2}} A D^{-\frac{1}{2}} = U\Lambda U^T$, with the diagonal matrix of eigenvalues of Λ and a diagonal degree matrix of D. To simplify the computation and matrix eigenvalue decomposition, g_θ is generally estimated by a truncated expansion using K^{th} Chebyshev polynomials $T_k(x)$ [26]:

$$g_{\theta'} \approx \sum_{k=0}^{K} \theta'_k T_k(\frac{2}{\lambda_{\max}} L - I_N) \tag{3}$$

where $\lambda_{\max}$ is the maximum eigenvalue in L. Take the conditions of $K = 1$, $\lambda_{\max} = 2$, $T_0(x) = 1$, $T_1(x) = x$

and $\theta'_0 = -\theta'_1 = \theta'$, then $g_{\theta'} \approx \theta'(I_N + D^{-\frac{1}{2}} A D^{\frac{1}{2}})$. Finally, the output of spectral convolution can be estimated as:

$$g_{\theta'} * \mathbf{x}^{t,temp} = \theta' \tilde{D}^{-\frac{1}{2}} \tilde{A} \tilde{D}^{-\frac{1}{2}} \mathbf{x}^{t,temp} \tag{4}$$

where A and D is renormalized by $\tilde{A} = A + I_N$ and $\tilde{D}_{ii} = \sum_j \tilde{A}_{ij}$, respectively. For the matrix inputs $\mathbf{X}^{temp} = (\mathbf{x}^{t-T_h+1,temp}, \cdots, \mathbf{x}^{t,temp}) \in \mathbb{R}^{mF \times T_h}$ of historical indoor multi-zone temperature values with stacking multiple convolutional layers, the output of spectral convolution for l-th layer $\mathbf{G}^l \in \mathbb{R}^{mF \times 1}$ can be calculated recursively as,

$$\mathbf{G}^{(1)} = g_{\theta'} * \mathbf{X}^{temp} = diag(\theta'^{(1)}) \tilde{D}^{-\frac{1}{2}} \tilde{A} \tilde{D}^{-\frac{1}{2}} \mathbf{X}^{temp} \tag{5}$$

$$\mathbf{G}^{(l+1)} = \sigma(diag(\theta'^{(l)}) \hat{A} \mathbf{G}^{(l)}) \tag{6}$$

where $\hat{A} = \tilde{D}^{-\frac{1}{2}} \tilde{A} \tilde{D}^{-\frac{1}{2}}$, $\mathbf{G}^{(l)}$ is the output of lth layer ($\mathbf{G}^{(0)} = \mathbf{X}^{temp}$), $\theta'^{(l)}$ contains the parameters in l-th layer, and $\sigma(\cdot)$ represents the sigmoid activation function. To avoid the gradient disappearance and overfitting with large numbers of graph convolutional layers, original input indoor temperature data are fused with the previous graph convolution outputs by weighting parameter of α to form the inputs of the layer graph convolution [27], [28],

$$\mathbf{G}^{(l+1)} = \sigma(\alpha \mathbf{X}^{temp} + (1-\alpha) \hat{A} \mathbf{G}^{(l)} \theta^{(l)}) \tag{7}$$

where α is the ratio of retaining the original information. Thus, both the local dependencies and neighbors' global dependencies can be preserved by the original information propagation of nodes. However, this may lead to redundant information and increase computational complexity. To address this problem, a 2D-convolutional layer is stacked as the output layer for L-layer GCN with the binary parameters $\mathbf{p} \in \mathbb{R}^L$ to select the latent spatially related features,

$$\mathbf{X}_{temp}^{GCN} = \sum_{l=1}^{L} p_l \mathbf{G}^{(l)} \tag{8}$$

if there exist no spatial dependencies for the lth graph convolution, $p_l = 0$, otherwise, $p_l = 1$. Fig. 5 shows the process of information propagation and feature selection in the proposed GCN. Similarly, the spatial features of multi-zone humidity can be extracted as follows.

$$\mathbf{X}_h^{GCN} = \sum_{l=1}^{L} p_l \mathbf{G}^{(l)} \tag{9}$$

One problem in the existing GCN-based module is the requirement of a predefined adjacent matrix A for the graph convolution operation. However, it is generally difficult to determine these matrices in different layers when extracting information with spatial correlation characteristics. In this section, a graph learning module is adopted to learn the adjacent matrix adaptively by the original data without any prior knowledge. For the case of multi-zone temperature with coupling spatial relationships, the graph is unidirectional and the graph adjacent matrix is asymmetric which is ensured by ReLU activation function. The latent spatial dependencies can be derived as follows,

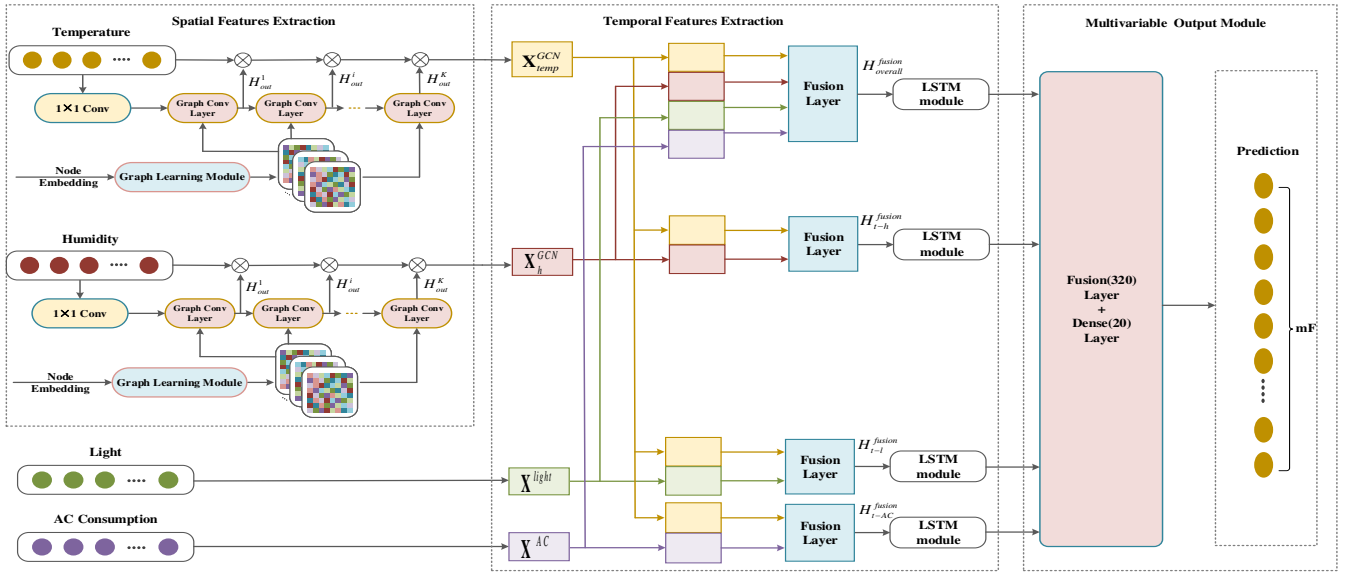$$\hat{A} = Softmax(ReLU(E_1 E_2^T - E_2 E_1^T)) \tag{10}$$

Fig. 4. The architecture of the proposed model (DL-GCN).

where $E_1, E_2 \in \mathbb{R}^{mF \times d}$ are randomly initialized source node embedding and target node embedding with d denotes a hyperparameter of the node embedding dimension. It is worth noting that the two node embedding matrices are updated during the model training process together with the model parameters.
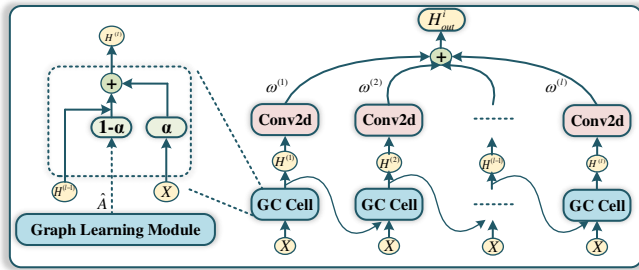

Fig. 5. The overall process of the graph convolution layer.

B. Temporal and Multivariable Coupling Features Extraction with Distributed LSTM Network

From the analysis in section II, the multi-zone indoor temperature is directly affected by some recent historical values, while several indirect variables also make an important influence on the future changes of indoor temperature. Therefore, a distributed information fusion framework based on LSTM is employed in this section to handle the long-term temporal correlation and the coupling features between the multiple variables, i.e., temperature, humidity, light, and AC power consumption, as shown in Fig. 3. The structure of the LSTM unit is shown in Fig. 6 with three gates, namely input gate, forget gate, and output gate. The forward computation

process is denoted as follows:

$$i_t = sigmoid(w_{xi}x_t + v_{hi}h_{t-1} + b_i) \quad (11)$$

$$f_t = sigmoid(w_{xf}x_t + v_{hf}h_{t-1} + b_f) \quad (12)$$

$$o_t = sigmoid(w_{xo}x_t + v_{ho}h_{t-1} + b_o) \quad (13)$$

$$c_t = f_t \circ c_{t-1} + i_t \circ tanh(w_{xc}x_t + v_{hc}h_{t-1} + b_c) \quad (14)$$

$$h_t = o_t \circ tanh(c_t) \quad (15)$$

where w and v are the weight matrices, b are the bias vector, tanh and sigmoid are two different activation functions, $\circ$ is an elementwise multiplication.
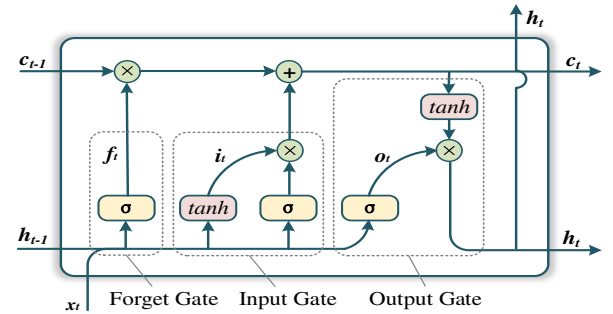
Fig. 6. LSTM memory block with one cell.

Here the temperature is regarded as the main feature and other variables are taken as the auxiliary features to excavate the internal relationships more intuitively [29]. The distributed information fusion is processed in two stages as shown in Fig. 5. In stage 1, the spatial features of humidity $\mathbf{X}_h^{GCN}$, input data of light and AC power consumption denoted as $\mathbf{X}^{light}$, $\mathbf{X}^{AC}$ are fused with the latent spatial characteristic from GCN output $\mathbf{X}_{temp}^{GCN}$ to further excavate the deep temporal information, coupling correlations between the primary variable (temperature) and each auxiliary variable (humidity, light, and AC power consumption), denoted as H_{t-h}^{fusion}, H_{t-l}^{fusion} and H_{t-AC}^{fusion}, respectively.

$$H_{t-h}^{fusion} = concat(\mathbf{X}_{temp}^{GCN}, \mathbf{X}_{h}^{GCN}) \qquad (16)$$

$$H_{t-l}^{fusion} = concat(\mathbf{X}_{temp}^{GCN}, \mathbf{X}^{light}) \qquad (17)$$

$$H_{t-AC}^{fusion} = concat(\mathbf{X}_{temp}^{GCN}, \mathbf{X}^{AC}) \qquad (18)$$

In stage 2, all the four types of characteristics are fused to extract the overall coupling correlation information between the primary variable and all the auxiliary variables. By this way, the complex coupling impact of the auxiliary variables on the indoor temperature can be fully extracted.

$$H_{overall}^{fusion} = concat(\mathbf{X}_{temp}^{GCN}, \mathbf{X}_{h}^{GCN}, \mathbf{X}^{light}, \mathbf{X}^{AC}) \qquad (19)$$

Next, the features from the four distributed fusion modules are handled by different LSTM networks, respectively to evacuate the temporal-spatial correlations and multivariable coupling characteristics among the main variables and auxiliary variables. Then the outputs of the four LSTM networks are concatenated by a feature fusion layer, which can be formulated as follows:

$$H^{fusion} = concat(H_{t-h}^{fusion}, H_{t-l}^{fusion}, H_{t-AC}^{fusion}, H_{overall}^{fusion}) \qquad (20)$$

After the concatenation layer, the fully connected dense layer with linear activation is employed to further explore the temporal-spatial and multivariable coupling features to output the prediction of the multi-zone indoor temperature. The output of the dense layer is defined as follows:

$$\mathbf{x}^{t+1,temp} = \mathbf{w}_{dense} H^{fusion} + \beta_{dense} \qquad (21)$$

where $\mathbf{w}_{dense}$ and β_{dense} are the weight matrices and bias vector in the dense layer, respectively, $\mathbf{x}^{t+1,temp}$ represents the predicted indoor room temperatures in the next time.

V. EXPERIMENTS

In this section, we use a real-world building dataset to validate the effectiveness of the proposed DL-GCN model by comparing with other baseline models. To validate the temporal-spatial correlation and multivariable coupling phenomenon of the multi-zone temperature, the effects of different extraction modules are analyzed by conducting ablation experiments.

A. Data Description

To verify the effectiveness of the proposed DL-GCN model, the operation dataset of an air-conditioned office building from Thailand named CUBEMS are used in this study [24]. Here three reasons are considered. First, the data were collected from a multi-zone large public building with 7 stories and 5 zones which is suitable for the multi-zone spatial features extraction. Second, the recorded data were collected with 1-minute intervals ranging from July 1, 2018 to December 31, 2019 with sufficient data points. Third, comprehensive data from the building are collected including the indoor environmental measurements and the electricity consumptions from the devices such as the individual air conditioning units, lighting, and plug loads in each zone.

B. Experimental Settings

1) Parameters Setup: The experiments were conducted using a computer equipped with an NVIDIA GeForce RTX 2060 GPU, an AMD Ryzen 5-3600 CPU (3.6GHz) and 16 GB RAM. The DL-GCN model is implemented in Python 3.6 with Pytorch 1.5.0 framework. All the selected data samples were divided into 60%, 20%, and 20% for training, validation, and testing, respectively. For all models, we utilize the past 2 hours' observed value to predict the next hour's data, thereby the lookup size T_h is set to 12. We set the batch size as 16 and the learning rate as 0.001. Mean square error (MSE) is selected as the loss function. The model is trained with early stopping strategy and optimized by Adam optimizer with iteratively updating the model parameters based on the gradient information. It should be noted that the proposed DL-GCN is an end-to-end deep learning architecture that the networks such as GCN and LSTMs are jointly trained for one loss function. The training process of the proposed DL-GCN is given below.

Algorithm 1 Training Algorithm: DL-GCN

Input: Original dataset ($\mathcal{X}_i \in \mathbb{R}^{N \times T_h \times mF \times 4}$, $\mathcal{Y}_i \in \mathbb{R}^{N \times mF \times 1}$), the objective function L, node set V, batch size n;

Output: The multi-zone temperature predictions $\mathbf{x}^{t+1,temp}$;

1: Initialize the hyper-parameters α, d, and the iteration number I. Divide the training set, validation set and test set, let $i = 1$. Randomly initialize the node embeddings E_1, E_2;

2: ***Repeat***

3:      Randomly select ith batch ($\mathcal{X}_i \in \mathbb{R}^{n \times T_h \times mF \times 4}$, $\mathcal{Y}_i \in \mathbb{R}^{n \times mF \times 1}$) from the original dataset;

4:      Calculate the graph adjacency matrix $\widehat{A} \in \mathbb{R}^{mF \times mF}$ by graph learning layer based on Eq.(9);

5:      Conduct graph convolution operation with batch temperature and humidity variable data ($\mathcal{X}_{i,temp} \in \mathbb{R}^{n \times T_h \times mF}$, $\mathcal{X}_{i,h} \in \mathbb{R}^{n \times T_h \times mF}$) to extract the spatial features;

6:      Use Eqs.(11)-(15) to extract the shallow temporal information by using the light, and AC power consumption data;

7:      Construct distributed fusion blocks to further excavate the deep spatial-temporal coupling correlation in Eqs.(16)-(19);

8:      Use the fusion and dense layers to determine the final output in Eqs.(20)-(21);

9:      Calculate the stochastic gradient, and update the node embeddings and model parameters according to their gradients and the learning rate;

10:      Let $i = i + 1$, go back to 3;

11: ***Until*** convergence or $i = I$ is reached.

---

2) Evaluation Metrics: Three metrics are selected to evaluate the model performance: Mean Absolute Error (MAE), Mean Square Error (MSE), and correlation coefficient (CORR). The definitions of these four metrics are given in Equations (21) to (23):
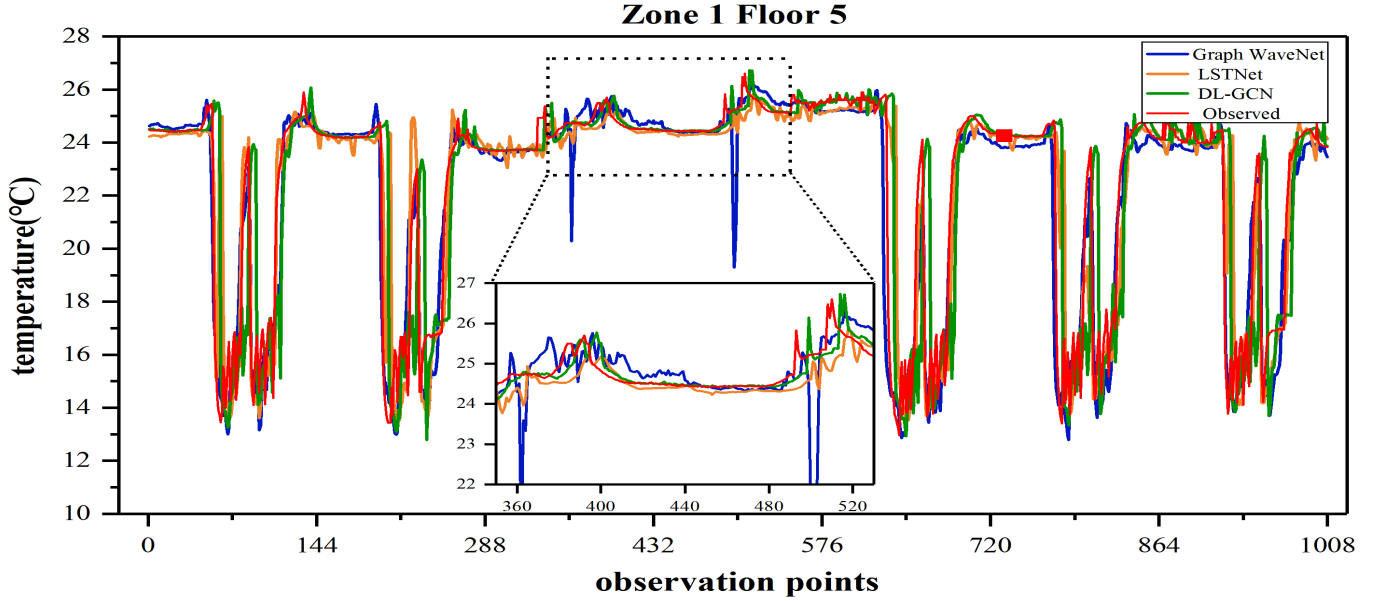
Fig. 7. A comparison of ground truth and predicted temperature values during one week by different models (Graph WaveNet, LSTNet, and DL-GCN).

$$MAE = \frac{1}{n} \sum_{i=1}^{n} |y_i - \hat{y}_i| \qquad (22)$$

$$MSE = \frac{1}{n} \sum_{i=1}^{n} (y_i - \hat{y}_i)^2 \qquad (23)$$

$$CORR = \frac{\sum_{i=1}^{n} (y_i - \overline{y_i})(\hat{y}_i - \overline{\hat{y}_i})}{\sqrt{\sum_{i=1}^{n} (y_i - \overline{y_i})^2 \sum_{i-1}^{n} (\hat{y}_i - \overline{\hat{y}_i})^2}} \qquad (24)$$

where y_i is the measured indoor temperature and $\hat{y}_i$ refers to the predicted indoor temperature by the proposed DL-GCN model, $\overline{y_i}$ and $\overline{\hat{y}_i}$ represent the mean of measured and predicted values, and n is the number of samples in the batch. Lower MAE and MSE represent better prediction results, and the CORR closer to 1 refers to the better fitting effect.

TABLE I
THE PERFORMANCE COMPARISON OF BASELINES AND DL-GCN.

Models	1-hour prediction			2-hour prediction		
	MAE	MSE	CORR	MAE	MSE	CORR
SVR	0.8099	2.2108	0.8642	1.0389	3.5267	0.7827
GRU	0.805	1.2714	0.8473	0.8792	1.3632	0.8216
MLP	0.9483	1.3035	0.8322	1.0871	1.4839	0.7754
LSTNet	0.5305	0.9545	0.9321	0.7232	1.7078	0.831
Graph WaveNet	0.613	0.9956	0.9022	0.6947	1.1566	0.8736
DL-GCN	**0.4769**	**0.7733**	**0.9597**	**0.6165**	**0.9705**	**0.9347**

3) Baselines: To illustrate the effectiveness and strength of our proposed DL-GCN model in multi-zone indoor temperature prediction with temporal-spatial correlation and multivariable coupling characteristics, five existing methods are chosen as the baseline models:

SVR [30]: Support Vector Regression (SVR) is a traditional machine learning method that widely utilized in time series prediction model. We choose the Radial Basis Function (RBF) kernel function to handle the nonlinear and high-dimensional problems in the experiments.

GRU [31]: Gate Recurrent Unit (GRU) is a popular variant of the RNNs with good performance to solve the gradient problems in long-term memory and back propagation.

MLP [32]: Multi-layer perceptron (MLP) is a classical neural network with a fully connected input layer, a hidden layer and an output layer.

LSTNet [33]: LSTNet integrates the CNN, RNN, and autoregressive modules to extract short-term and long-term temporal patterns.

Graph WaveNet [34]: Graph WaveNet is a method with both graph convolution and dilated casual convolution to extract the hidden temporal-spatial dependencies automatically.

C. Experimental Results

1) Comparison with Baseline Models: After the training and cross-validation process, the trained DL-GCN model and five baseline models are applied to the testing dataset. The average values of these model-predicted results from 10 training times are taken as the final experimental results. The evaluation results of all the above-mentioned methods are listed in Table I. The indoor temperatures from multi-zone on two different future time points (the next 6-step point and 12-step point) are predicted.

According to Table I, the longer the prediction length, the larger of model errors for all six models. Furthermore, the proposed DL-GCN model outperforms all the baseline models with all three metrics. More specifically, the average MSE values of the baseline models increase 185.89%, 64.41%, 68.56%, 23.43%, and 28.75% relative to the DL-GCN when predicting the next 6-step multi-zone indoor temperatures.

Among the five baseline models, the classical machine learning SVR model provides the worst model accuracy with evident larger MSE values in both prediction cases. The prediction results of the deep learning methods such as MLP and GRU are greatly improved because of the consideration of temporal feature extraction in the network. However, there is a clear gap in comparison with the proposed DL-GCN for all the metrics due to the lack of exploring the spatial correlations between multiple zones. The performance of LSTNet and Graph WaveNet is the closest to that of DL-GCN. The LSTNet employs the convolution network and recurrent skip network to capture the short-term and long-term temporal patterns but ignores the spatial features, and the Graph WaveNet model captures the temporal-spatial dependencies simultaneously by stacking the graph convolution module and the temporal convolution module. However, neither of them considers the coupling features between multiple variables therefore their prediction performance is less accurate than the proposed DL-GCN model. That is due to the fact that the GCN, LSTM, and distributed information fusion framework in the proposed DL-GCN are able to facilitate the extraction of the spatial, temporal, and multivariable coupling features extraction such that the prediction accuracy of multi-zone indoor temperature can be improved. In addition, to visualize the prediction results from different models, the experimental results from a time slice (over one week, 2019/9/12 to 2019/9/18) with 1008 sequential observed points are illustrated in Fig. 7. It should be noted that only two outstanding baseline models with higher accuracy (LSTNet and Graph WaveNet) are compared with the proposed DL-GCN model in the figure. It is evident that the proposed DL-GCN model can track the varying trends including the periodic changes during the weekdays and special changes during weekends of indoor temperature from multiple zones with higher prediction accuracy. It confirms that the consideration of multivariable coupling from different zones can help to improve the performance when modeling the multi-zone indoor temperature.

TABLE II
THE PERFORMANCE COMPARISON OF DIFFERENT DL-GCN VARIANTS.

Models	MAE	MSE	CORR
DL	0.5961	0.8781	0.9483
GCN	0.5715	0.8701	0.9481
L-GCN	0.5437	0.8529	0.9438
DL-GCN(T)	0.4836	0.7936	0.9540
DL-GCN	**0.4769**	**0.7733**	**0.9597**

2) Ablation Experiments: To demonstrate the effectiveness of the special components in our proposed model, we conduct ablation experiments by comparing different variants of DL-GCN. The details of the variants are as follows.

DL: It removes the spatial information extraction module to learn the strong coupling relationship between multiple variables taking advantage of the distribution fusion framework.

GCN: It removes the temporal information extraction module to learn the latent spatial correlations between multizone variables utilizing the graph convolution module with adaptively updating weights of neighbor nodes.

L-GCN: It replaces the distribution fusion LSTM framework with an original LSTM layer to learn the temporal dependencies.

DL-GCN (T): It take the temperature only as the inputs of GCN. And the humidity, light, and AC power consumption are directly put into the temporal features extractions.

It is notable that all the variant models are with the same settings as DL-GCN. The experiments are carried out based on data from two adjacent zones on three consecutive days. We list the prediction errors on the next 6-step point, as shown in Table II. The DL model suffers the most serious performance degradation than other models, indicating that spatial feature extraction is quite necessary for multi-zone indoor temperature prediction. Assisted by the GCN networks, the GCN and L-GCN models provide better prediction accuracy, but are still far lower than the proposed DL-GCN. It is evident that DL-GCN(T) and the proposed DL-GCN outperforms all its variants significantly in terms of MAE, MSE, and CORR. The DL-GCN is providing slightly better results than DL-GCN(T). The DL-GCN(T) can also be chosen sometimes. It therefore confirms that the effectiveness and efficiency of the spatial, temporal and distributed information fusion modules in multizone indoor temperature prediction for large-scale buildings.

3) Effect of Hyperparameters: In this section, we investigate the effect of hyperparameters including the epoch number I and node embedding dimension d. The varying ranges of I and d are set up from 50 to 150 with the interval 10, and from 30 to 50 with the interval 5, respectively. The experimental results for the epoch number with the MSE and MAE are shown in Fig. 8(a). It can be seen that as the number of iterations increases, the MSE and MAE are gradually decreased to the minimal values until the iterations number reaches 120. Therefore, to reduce the training cost, we choose the iterations number of 120 in the experiments.

Fig. 8(b) depicts the experimental results for the dimension of node embedding. It can be drawn that both the MSE and MAE are approaching the minimum values when the node embedding dimension is 35. Hence, it is set as 35 to reduce the computational complexity while ensuring the reliability of the prediction results.
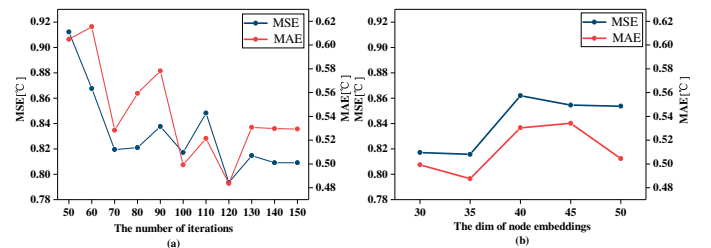

Fig. 8. Performance of models using the different parameter configurations.

VI. CONCLUSIONS

In this paper, a novel deep learning architecture incorporating distributed LSTM and GCN named DL-GCN has been developed to predict the multi-zone indoor temperature in largescale buildings. With the graph self-learning GCN module,

the spatial features between multi-zone indoor temperatures were explored, and the temporal correlation and multivariable coupling characteristics were extracted by distributed LSTM networks. The proposed DL-GCN model was compared with existing models using datasets from a real large-scale building. The comparison results confirm that the proposed DL-GCN model outperforms the other models with smaller MAE and MSE, higher correlation coefficients. Further, the ablation experiment results have demonstrated the benefits of spatial, temporal, and distributed information fusion modules in multi-zone indoor temperature prediction for large-scale buildings. In future study, the optimal regulation strategy for HVAC systems in large-scale buildings will be developed with the indoor temperature forecasting results. Moreover, the forecasting results can also be used to develop a demand response scheme for some building communities powered by renewable energy so that the fluctuating renewable energy can be fully used.

REFERENCES

[1] Y. Yang, S. Srinivasan, G. Hu, and C. J. Spanos, "Distributed control of multizone hvac systems considering indoor air quality," *IEEE Transactions on Control Systems Technology*, vol. 29, no. 6, pp. 2586–2597, 2021.

[2] B. Li, W. Cai, and X. Liu, "A novel min-consensus-based distributed control method for multi-zone ventilation systems," *IEEE Transactions on Industrial Electronics*, vol. 69, no. 8, pp. 8284–8295, 2022.

[3] E. Rezaei and H. Dagdougui, "Optimal real-time energy management in apartment building integrating microgrid with multizone hvac control," *IEEE Transactions on Industrial Informatics*, vol. 16, no. 11, pp. 6848–6856, 2020.

[4] T. Wei, S. Ren, and Q. Zhu, "Deep reinforcement learning for joint datacenter and hvac load control in distributed mixed-use buildings," *IEEE Transactions on Sustainable Computing*, vol. 6, no. 3, pp. 370–384, 2021.

[5] P. Hietaharju, M. Ruusunen, and K. Leivisk, "A dynamic model for indoor temperature prediction in buildings," *Energies*, vol. 11, no. 6, p. 1477, 2018.

[6] S. Alawadi, D. Mera, M. Fernndez-Delgado, F. Alkhabbas, C. M. Olsson, and P. Davidsson, "A comparison of machine learning algorithms for forecasting indoor temperature in smart buildings," *Energy Systems*, vol. 13, no. 3, pp. 689–705, 2020.

[7] X. Zhang, Y. Lei, H. Chen, L. Zhang, and Y. Zhou, "Multivariate time series modeling for forecasting sintering temperature in rotary kilns using dcgnet," *IEEE Transactions on Industrial Informatics*, vol. 17, no. 7, pp. 4635–4645, 2020.

[8] S. Zhang, Y. Guo, P. Zhao, C. Zheng, and X. Chen, "A graph-based temporal attention framework for multi-sensor traffic flow forecasting," *IEEE Transactions on Intelligent Transportation Systems*, vol. 23, no. 7, pp. 7743–7758, 2021.

[9] Z. Afroz, T. Urmee, G. M. Shafiullah, and G. Higgins, "Real-time prediction model for indoor temperature in a commercial building," *Applied Energy*, vol. 231, pp. 29–53, 2018.

[10] H. Alasha'Ary, B. Moghtaderi, A. Page, and H. Sugo, "A neuro-fuzzy model for prediction of the indoor temperature in typical australian residential buildings," *Energy and Buildings*, vol. 41, no. 7, pp. 703–710, 2009.

[11] F. Mateo, J. J. Carrasco, A. Sellami, M. Millan-Giraldo, M. Dominguez, and E. Soria-Olivas, "Machine learning methods to forecast temperature in buildings," *Expert Systems with Applications*, vol. 40, no. 4, pp. 1061–1068, 2013.

[12] G. Lewenfus, W. A. Martins, S. Chatzinotas, and B. Ottersten, "Joint forecasting and interpolation of time-varying graph signals using deep learning," *IEEE Transactions on Signal and Information Processing over Networks*, vol. 6, pp. 761–773, 2020.

[13] N. Jin, Y. Zeng, K. Yan, and Z. Ji, "Multivariate air quality forecasting with nested lstm neural network," *IEEE Transactions on Industrial Informatics*, vol. 17, no. 12, pp. 8514–8522, 2021.

[14] S. Du, T. Li, Y. Yang, and S. J. Horng, "Deep air quality forecasting using hybrid deep learning framework," *IEEE Transactions on Knowledge and Data Engineering*, vol. 33, no. 6, pp. 2412–2424, 2019.

[15] L. Jiang, X. Wang, W. Li, L. Wang, and L. Jia, "Hybrid multitask multi-information fusion deep learning for household short-term load forecasting," *IEEE Transactions on Smart Grid*, vol. 12, no. 6, pp. 5362–5372, 2021.

[16] Z. Fang, N. Crimier, L. Scanu, A. Midelet, and B. Delinchant, "Multi-zone indoor temperature prediction with lstm-based sequence to sequence model," *Energy and Buildings*, vol. 245, p. 111053, 2021.

[17] C. Xu, H. Chen, J. Wang, Y. Guo, and Y. Yuan, "Improving prediction performance for indoor temperature in public buildings based on a novel deep learning method," *Building and Environment*, vol. 148, pp. 128–135, 2019.

[18] W. Lin, D. Wu, and B. Boulet, "Spatial-temporal residential short-term load forecasting via graph neural networks," *IEEE Transactions on Smart Grid*, vol. 12, no. 6, pp. 5373–5384, 2021.

[19] Z. Cui, K. Henrickson, R. Ke, and Y. Wang, "Traffic graph convolutional recurrent neural network: A deep learning framework for network-scale traffic learning and forecasting," *IEEE Transactions on Intelligent Transportation Systems*, vol. 21, no. 11, pp. 4883–4894, 2020.

[20] L. Zhao, Y. Song, C. Zhang, Y. Liu, and H. Li, "T-gcn: A temporal graph convolutional network for traffic prediction," *IEEE Transactions on Intelligent Transportation Systems*, vol. 21, no. 9, pp. 3848–3858, 2019.

[21] Y. Qi, Q. Li, H. Karimian, and D. Liu, "A hybrid model for spatiotemporal forecasting of pm2.5 based on graph convolutional neural network and long short-term memory," *Science of The Total Environment*, vol. 664, pp. 1–10, 2019.

[22] K. Mahdi and J. Wang, "Spatio-temporal graph deep neural network for short-term wind speed forecasting," *IEEE Transactions on Sustainable Energy*, vol. 10, no. 2, pp. 670–681, 2018.

[23] S. Guo, Y. Lin, H. Wan, X. Li, and G. Cong, "Learning dynamics and heterogeneity of spatial-temporal graph data for traffic forecasting," *IEEE Transactions on Knowledge and Data Engineering*, vol. 34, no. 11, pp. 5415–5428, 2021.

[24] P. Manisa, C. Gopal, S. Jitkomut, A. Chaodit, P. Wanchalerm, S. Surapong, A. Kulyos, and H. Naebboon, "Cu-bems, smart building electricity consumption and indoor environmental sensor datasets," *Scientific Data*, vol. 7, no. 241, 2020.

[25] J. Bruna, W. Zaremba, A. Szlam, and Y. Lecun, "Spectral networks and locally connected networks on graphs," *Computer Science*, 2013.

[26] T. N. Kipf and M. Welling, "Semi-Supervised Classification with Graph Convolutional Networks," *arXiv e-prints*, p. arXiv:1609.02907, Sept. 2016.

[27] Z. Wu, S. Pan, G. Long, J. Jiang, X. Chang, and C. Zhang, "Connecting the dots: Multivariate time series forecasting with graph neural networks," *The 26th ACM SIGKDD Conference on Knowledge Discovery and Data Mining*, 2020.

[28] S. Guo, Y. Lin, N. Feng, C. Song, and H. Wan, "Attention based spatial-temporal graph convolutional networks for traffic flow forecasting," in *The 33rd AAAI Conference on Artificial Intelligence (AAAI)*, 2019.

[29] X. Yi, J. Zhang, Z. Wang, T. Li, and Z. Yu, "Deep distributed fusion network for air quality prediction," in *The 24th ACM SIGKDD International Conference*, 2018.

[30] Z. Fan, D. Chirag, L. SiewEang, Y. Junjing, and S. KwokWei, "Time series forecasting for building energy consumption using weighted support vector regression with differential evolution optimization technique," *Energy and Buildings*, vol. 126, pp. 94–103, 2016.

[31] W. Lulu, Z. Kaile, and Y. Shanlin, "Load demand forecasting of residential buildings using a deep learning model," *Electric Power Systems Research*, vol. 179, p. 106073, 2020.

[32] A. Nivine, S. Isam, and Y. Rafic, "Smart building: Use of the artificial neural network approach for indoor temperature forecasting," *Energies*, vol. 11, no. 2, p. 395, 2018.

[33] G. Lai, W. Chang, Y. Yang, and H. Liu, "Modeling long- and short-term temporal patterns with deep neural networks," *ACM*, 2018.

[34] Z. Wu, S. Pan, G. Long, J. Jiang, and C. Zhang, "Graph wavenet for deep spatial-temporal graph modeling," *Twenty-Eighth International Joint Conference on Artificial Intelligence IJCAI-19*, 2019.